ISSN 1027-4510, Journal of Surface Investigation: X-ray, Synchrotron and Neutron Techniques, 2016, Vol. 10, No. 5, pp. 1096–1100. © Pleiades Publishing, Ltd., 2016.
Original Russian Text © V.A. Novikov, D.V. Grigoryev, A.V. Voitsekhovskii, S.A. Dvoretsky, N.N. Mikhailov, 2016, published in Poverkhnost', 2016, No. 10, pp. 108–112.

Investigation of the Surface-Potential Distribution of Epitaxial CdHgTe Films

V. A. Novikov[a], *, D. V. Grigoryev[a], A. V. Voitsekhovskii[a], S. A. Dvoretsky[b], and N. N. Mikhailov[b]

[a] *Tomsk State University, Tomsk, 634050 Russia*

[b] *Rzhanov Institute of Semiconductor Physics, Siberian Branch, Russian Academy of Sciences, Novosibirsk, 630090 Russia*

**e-mail: novikovvadim@mail.ru*

Received February 5, 2016

Abstract—The epitaxial growth of CdHgTe films is accompanied by the formation of *V* defects whose density and electronic properties greatly affect the characteristics of a terminal device based on the given material. Scanning atomic-force microscopy techniques are proposed to investigate how electronic properties vary in the *V*-defect region of an epitaxial CdHgTe film. It is experimentally demonstrated that variations in the component composition of individual crystallites generating *V* defects create not only the complex spatial distribution of a potential field but also a potential barrier along the crystallite periphery. The given barrier must alter the charge-carrier exchange between crystallites, appreciably changing the current distribution over the *V*-defect area.

Keywords: epitaxial films, surface potential, *V* defects, atomic-force microscopy

DOI: 10.1134/S1027451016050372

INTRODUCTION

Among materials used to create infrared (IR) photoconverters, the leading position is occupied by epitaxial structures based on $Cd_xHg_{1-x}Te$ (CMT) solid solutions [1]. First of all, this is related to high-speed operation and a large quantum efficiency in the covered wavelength range. The main disadvantages of epitaxial CMT films are polycrystalline phase inclusions that are usually called *V* defects [2]. Hence, with the aim of attaining the high performance of CMT photoconverters, it is necessary to ensure homogeneous electric properties of the initial material, i.e., reduce both the *V*-defect density and/or their negative influence on the electrophysical parameters of final products.

After *V* defects appear in an epitaxial CMT film, the electrical properties become inhomogeneously distributed over the entire film bulk. This is associated with the fact that *V* defects are macrodefects (i.e., ensembles of crystallites) with lengths in the range of 5–20 μm. Their transverse sizes alter from 0.2 to 1.5 μm. It was demonstrated [2–11] that, in the *V*-defect region, the solid-solution composition differs from the epitaxial-film one. However, there are significant contradictions in the experimental data on the elemental composition of *V* defects. For example, with the help of X-ray spectral analysis, the authors of [5, 6] revealed that the excess of tellurium reaches 3% in the epitaxial-film regions with a high *V*-defect concentration. At the same time, electron-probe X-ray microanalysis data indicate that, in the *V*-defect area, the mercury content increases by 6 at % [11]. In [4, 10], the Kelvin probe force microscopy (KPFM) was used to investigate the spatial distribution of electronic properties over the *V*-defect region of the epitaxial CMT film. Analysis of the results revealed that V defects are distinguished by a higher content of mercury.

In connection with the forgoing, the goal of this work is to determine how the electrophysical characteristics of the epitaxial CMT-film surface are distributed over the *V*-defect region. To implement the goal mentioned above, the KPFM, scanning capacitance microscopy (SCM), scanning spreading resistance microscopy (SSRM), and energy-dispersive analysis (EDA) are employed to comprehensively investigate the spatially distributed electronic properties and the elemental composition of epitaxial CMT films in the *V*-defect region.

EXPERIMENTAL

Heteroepitaxial *n*-type CMT films, which were grown on (013)-oriented GaAs substrates with ZnTe and CdTe buffer layers by means of molecular-beam epitaxy, were investigated. Epitaxial structures were grown at the Rzhanov Institute of Semiconductor Physics, Siberian Branch, Russian Academy of Sciences.

The distribution of electronic properties over the surface was studied by measuring the spatial distribu-

tions of the surface potential and capacitive contrast with the help of Kelvin probes and SCM. In addition, the conductivity distributions over separate *V*-defect areas were measured via SSRM. Measurements were carried out by means of an NT–MDT (Zelenograd) Solver HV atomic-force microscope (AFM) under normal conditions. Boron-doped platinum-coated probes based on polycrystalline silicon, namely, NT–MDT NSG11/Pt probes, were employed. In the *V*-defect region, the elemental composition of the epitaxial CMT films was examined using a Quanta 3D scanning electron microscope equipped with an EDA system.

To obtain the surface-potential profile, the contact-potential difference (CPD) distribution between the AFM probe-needle tip and the epitaxial-film surface was measured. With the aim of eliminating the influence of the surface relief, the KPFM was implemented as the two-pass technique. During the first pass (or scanning), the surface profile is recorded under semicontact conditions. Afterward, the probe is lifted at distance z of about 50–100 nm [12], and the dc and ac voltages (U_0 and $U_1\sin(\omega t)$, respectively) are applied between the probe and the surface. Voltage supply to the probe and the surface excites the electric force of interaction, the Z component of which can be written as

$$F_z = -\left[\frac{1}{2}\left(\left[U_0 - U_{\mathrm{CPD}}(x,y)\right]^2 + \frac{1}{2}U_1^2\right) + (U_0 - U_{\mathrm{CPD}}(x,y))U_1\sin(\omega t) - \frac{1}{4}U_1^2\cos(2\omega t)\right]\frac{\partial C}{\partial z}, \quad (1)$$

where $U_{\mathrm{CPD}}(x, y)$ is the CPD between the cantilever's needle tip and the surface at the point (x, y) and C is the electrical capacitance accumulated in the air gap z between the cantilever's needle tip and the surface.

According to the KPFM, the interaction force $F_{z1\omega}$ is recorded on the ac first harmonic; i.e., the interaction force is described by the second summand in expression (1). Therefore, at a constant probe voltage of $V = U_{\mathrm{CPD}}(x, y)$, the interaction force is zero ($F_{z1\omega} = 0$) and the cantilever ceases harmonic oscillations, as is recorded by the feedback system. During the scanning process, the needle's dc voltage is selected at each measurement point. The distribution of compensating voltages applied to the needle is commonly called the surface-potential distribution.

SCM is analogous to the KPFM. In the former approach, signals are recorded at the second harmonic of an excitation signal. As a result, the interaction force between the probe and the surface can be written as

$$F_{z2\omega} = \frac{1}{4}U_1^2\cos(2\omega t)\frac{\partial C}{\partial z}. \quad (2)$$

As is seen from expression (2), the recorded interaction force is proportional to the change in the capacitance of the air gap between the probe and the surface. The interaction force varies with charge stored in the probe–surface distance. As a result, the cantilever's oscillation amplitude undergoes changes due to the action of the electric force. Since the electronic properties of the cantilever remain constant, the observed variations can be related only to changes in the space charge in the material's surface region. When the charge is inhomogeneously distributed over the semiconductor surface, e.g., in the *p–n* junction region [13, 14], changes in component $\partial C/\partial z$ lead to variations in the cantilever's oscillation amplitude. Thus, the resultant capacitive-contrast distribution is determined by the amount of charge at the investigated sample surface, which is independent of the CPD.

In the case where the applied probe–sample bias is constant, SSRM enables us to obtain the current-strength distribution maps in the sample. Since the voltage remains invariable during the measurement process, a change in current strength characterizes the distribution of inhomogeneous resistance over the sample. During the course of studies of *V* defects in the CMT film, a series of AFM images was recorded by varying the needle voltage from 0 to –10 V with a step of 1 V.

EXPERIMENTAL RESULTS

The performed investigations made it possible to obtain AFM images of the CPD distribution in the *V*-defect region (Fig. 1). It follows from Fig. 1b that CPDs possess different values in the *V*-defect area and at the epitaxial CMT-film surface. The CPD distribution is highly inhomogeneous in the *XY*-plane of the *V*-defect region. Since the CPD measured via the KPFM depends on the electronic properties of a material, its observable inhomogeneous distribution defines a local change in the work function of the CMT surface.

As is seen in Fig. 1, two types of CPD distribution can be conventionally recognized in the *V*-defect region, one of which corresponds to individual crystallites and another, the intergranular-space region. It was previously demonstrated that the CPD measured by means of the KPFM depends on the difference between the work functions of the probe and the material under study.

Since the work function of the probe is constant during measurements, the ascertained changes can be caused by variations in the local work function of the material. However, in the analysis of the obtained data, it is necessary to allow for the bending of energy bands arising in the semiconductor's surface region. When band bending is modeled on the semiconductor surface, it is possible to note two extreme cases: with and without Fermi-level pinning in the semiconductor's near-surface region.

In the case where the effect of Fermi-level pinning at the surface is not taken into account, the system under measurement can be considered a metal–semiconductor contact with an air gap. Then, the CPD can be expressed as

$$\Delta\varphi = \varphi_m - (\chi + \varphi_s + \varphi_n),$$

where φ_m is the work function of the probe, χ is the semiconductor's electron affinity, φ_s is the band bending on the semiconductor surface, and φ_n is the energy gap between the conduction-band bottom and the Fermi level in the semiconductor volume. Quantities φ_m and φ_n are independent of the applied bias and solid-solution composition, χ is determined only by the component composition of the material under study, and φ_s is the applied bias. Therefore, the inhomogeneities observed in the CPD distribution can be induced only by variations in the component composition of the material and/or the amount of band bending on the surface.

To eliminate the dependence between band bending in the surface region of a CMT film and the measurement conditions, an additional dc or ac bias was created between the sample and the probe. The measured quantity was not varied by the supplied bias. Therefore, quantity φ_s is independent of the external bias applied to the probe. Thus, the observable change in the *V*-defect region is related to a variation in the component composition of the CMT film.

Let us assume that, in the *XY*-plane, the CPD increment with respect to the epitaxial CMT film, namely, ΔCPD, can be represented as the difference between the average electron affinity of the epitaxial film, χ_{film}, and the electron affinity of an individual crystallite, χ_i. The electron affinity of the CMT film depends on the solid-solution composition. Then, with allowance for the expression from [15], quantity ΔCPD can be defined as

$$\Delta\text{CPD} = [1.29 - 7.13\times10^{-4}T](x_1 - x_2) - 0.54(x_1^2 - x_2^2) + 0.56(x_1^3 - x_2^3), \quad (3)$$

where x_1 and x_2 are the solid-solution component contents at the chosen points. It was demonstrated [16] that, on average, the CPD inherent to the *V*-defect area is 50 mV greater than that of the epitaxial film. Hence, further calculations are performed for the given value of ΔCPD. At a molar content of cadmium of $x_1 = 0.22$ and $x_2 = 0.166$ in the epitaxial CMT film and $\Delta\text{CPD} = 0.05$ mV; i.e., the average CdTe content decreases by 0.054. Therefore, *V* defects are generated predominantly by crystallites with an increased mercury content and invariable tellurium concentration.

The measured quantity ΔCPD depends only on the material composition if the Fermi level is rigidly fixed on the surface. It can be assumed that, in the CMT film, charge-neutrality-level position depends linearly on the solid-solution composition [16]. Hence, at

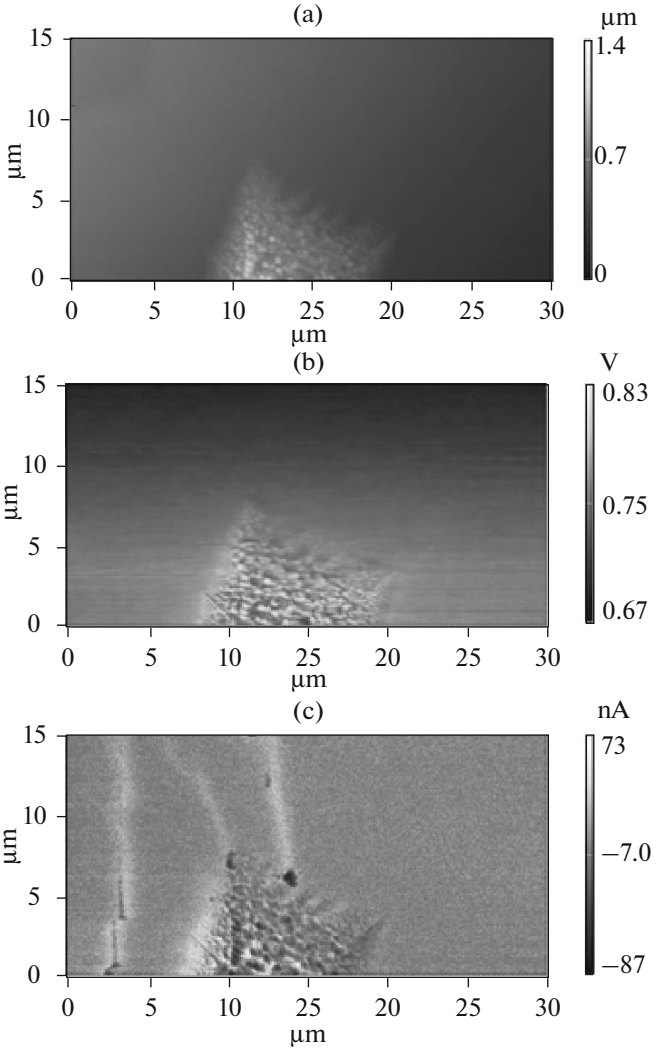

Fig. 1. AFM images of the (a) morphology, (b) CPD distribution, and (c) capacitive contrast in the epitaxial *n*–CdHgTe film.

$\Delta\text{CPD} = 0.05$ mV, the material composition must be altered by 0.076 toward an increase in the HgTe content of the CMT solid solution.

It is evident from the above results that, on average, the CMT solid-solution composition should vary from 0.054 to 0.076 depending on which mechanism is implemented to a larger extent. To exclude the measured CPD from being affected by alterations in the molar fraction of tellurium, the material's component composition was investigated by means of EDA. The results demonstrated that the Te content remains practically the same in both the *V*-defect area and the epitaxial CMT film.

From the above discussion, it is apparent that the CPD undergoes variations at the interface of individuals crystallites (Fig. 1). As is seen in Fig. 1c, the capacitance conforming to the probe–surface distance alters along the periphery of crystallites and conglom-

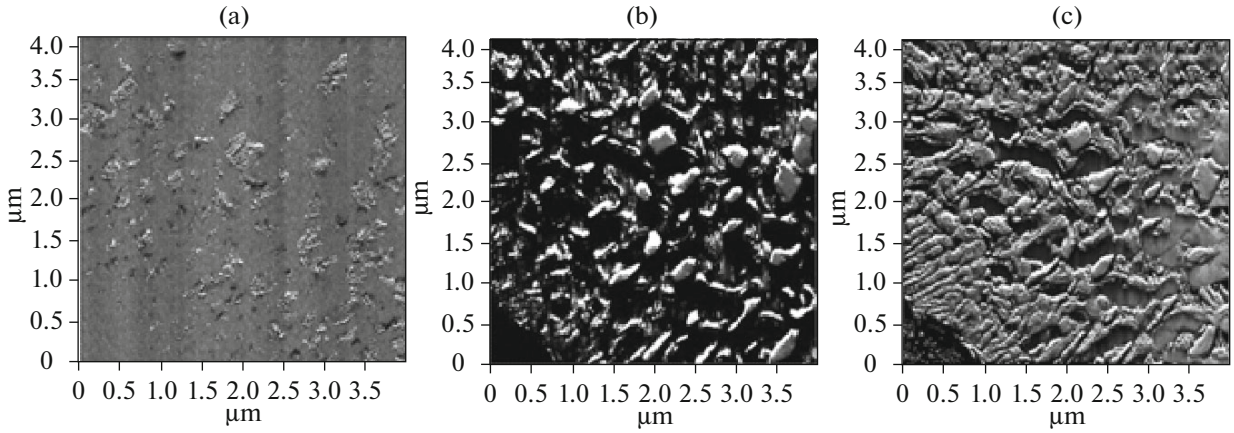

Fig. 2. AFM images of the current-strength distributions over the *V*-defect area at voltages of (a) 0, (b) −5, and (c) −10 V.

erates; i.e., it can be said that the spatial-charge region is observed at the periphery of each individual grain. In addition, it is clear that quantity dC/dz is independent of changes in the component composition. On account of charges existing in the surface region of the CMT film, additional band-bending regions on the surface must be formed and, consequently, current-flow process must undergo variations.

AFM images of the current-strength distributions, which were obtained at constant probe voltages, are presented in Fig. 2. It is evident that, in the absence of external bias, a current traverses isolated crystallites. This implies that the photocurrent arising from red-laser radiation scattering at the semiconductor surface flows through individual crystallites. We note that the given radiation is reflected from the bar of the probe used to record the working signal.

An increase in external bias alters both the distribution of the flowing current and its value. The periphery of separate grains does not carry a current. This is evidence of a potential barrier. Analysis of the dependence between the conducting area of the grains and the applied voltage revealed that the *V*-defect area increases almost linearly with increasing external bias. At a probe voltage of −10 V, the conducting surface area is approximately 60% of the total area under study. It is pertinent to note that measurements were carried out at room temperature when the semiconductor is strongly degenerate. Hence, it can be assumed that, at working temperatures (about 77 K) typical of the practical use of device structures based on CMT films, the total area contributing to the current can differ from that corresponding to 300 K.

CONCLUSIONS

From studying the distribution of the surface's electronic properties in the *V*-defect region of an epitaxial $Cd_xHg_{1-x}Te$ film, it is revealed that the spatial distributions of the contact-potential difference and capacitive contrast are inhomogeneous. The spatial distribution of the CPD indicates that, in the case of *V* defects, its value differs from that of the main matrix of the material. The observed difference is caused by the fact that *V* defects are characterized by an enhanced content of mercury atoms.

The electrically conductive surface area of the *V*-defect region within the epitaxial CMT film varies almost linearly upon the supply of an external bias and attains 60% if the needle voltage and temperature are −10 V and 300 K, respectively. The inhomogeneous current distribution over the *V*-defect area is related to an additional potential barrier arising along the periphery of individual crystallites or their conglomerates,

ACKNOWLEDGMENTS

This work (research grant 8.2.10.2015) was supported by the Tomsk State University Academic D.I. Mendeleev Fund Program for 2015.

REFERENCES

1. A. Rogal'skii, *Infrared Detectors* (Nauka, Novosibirsk, 2003) [in Russian].
2. V. N. Ovsyuk, G. L. Kuryshev, Yu. G. Sidorov, et al., *Matrix Photodetector Infrared Devices* (Nauka, Novosibirsk, 2001) [in Russian].
3. E. V. Permikina, A. S. Kashuba, and V. V. Arbenina, Inorg. Mater. **48** (7), 1134 (2012).
4. V. A. Novikov, D. V. Grigoryev, D. A. Bezrodny, and S. A. Dvoretsky, Appl. Phys. Lett. **105** (10), 1063 (2014).
5. Yu. G. Sidorov, S. A. Dvoretskii, V. S. Varavin, N. N. Mikhailov, M. V. Yakushev, and I. V. Sabinina, Semiconductors **35** (9), 1134 (2001).
6. S. N. Yakunin and N. N. Dremova, JETP Lett. **87** (9), 1134 (2008).

7. T. Aoki, Y. Chang, G. Badano, J. Zhao, C. Grein, S. Sivananthan, and D. J. Smith, J. Cryst. Growth **265**, 1016 (2004).
8. E. V. Permikina, A. S. Kashuba, and I. A. Nikiforov, Usp. Prikl. Fiz. **1** (4), 510 (2013).
9. T. Aoki, D. J. Smith, Y. Chang, J. Zhao, G. Badano, C. Grein, and S. Sivananthan, Appl. Phys. Lett. **82**, 1063 (2003).
10. V. A. Novikov and D. V. Grigor'ev, Semiconductors **49** (3), 309 (2015).
11. A. S. Kashuba, A. V. Zablotskii, E. V. Korostylev, et al., Vestn. MITKHT **5** (5), 19 (2010).
12. O. Vatel and M. Tanimoto, J. Appl. Phys. **77** (6), 1063 (1995).
13. W. Melitz, J. Shen, A. Kummel, and S. Lee, Surf. Sci. Rep. **66**, 1016 (2011).
14. S. B. Kuntze, D. Ban, E. H. Sargent, St. J. Dixon-Warren, J. K. White, and K. Hinzer, Crit. Rev. Solid State Mater. Sci **30** (2), 1080 (2007).
15. A. V. Voitsekhovskii, D. I. Gorn, I. I. Izhnin, A. I. Izhnin, V. D. Goldin, et al., Izv. Vyssh. Uchebn. Zaved., Fiz. **55** (8), 50 (2012).
16. V. N. Brudnyi and S. N. Grinyaev, Semiconductors **35**, 784 (2001).

Translated by S. Rodikov